

Self trapping from degenerate bands (spin $S = 1$) and related phenomena

F. V. Kusmartsev and É. I. Rashba

L. D. Landau Institute of Theoretical Physics, USSR Academy of Sciences

(Submitted 16 August 1983)

Zh. Eksp. Teor. Fiz. **86**, 1142–1155 (March 1984)

A theory of the self-trapping barrier in crystal with degenerate bands (spin $S = 1$) is developed for holes and Frenkel excitons. It is shown that band degeneracy leads to spontaneous symmetry breaking of the barrier, which acquires a prolate or oblate shape. The dependence of the barrier height on a number of parameters, such as the ratio of the effective masses, the deformation potentials, and others is investigated. The barrier-height scale is determined in all cases by the mass of the heavy hole (exciton). The mechanism of formation of quasimolecular self-trapped holes and excitons is discussed. Similar results were obtained for the strong-coupling polaron, for which lowering of the symmetry leads to the appearance of two rotational degrees of freedom. The results are applied to a number of other problems: fluctuation levels in semiconductors, the Urbach rule, and others. It is shown also that in systems with multicomponent order parameters the critical nuclei may be nonspherical (e.g., cigar- or disk-shaped).

1. INTRODUCTION

Most theoretical studies of self-trapping (ST) in crystals are based on models in which the electron (hole, exciton) spectrum is nondegenerate. Yet almost in all experimental observations the ST is from degenerate bands^{1,2} (among the few exceptions are ST in systems with quasi-one-dimensional spectra, in pyrene, in liquid He). This rule does not lend itself to a clear and sufficiently general theoretical interpretation. In fact, since the ST states have practically always a spatial scale of the order of the lattice constant, they cannot be described in a continual approximation. In particular, one cannot apply to them the effective-mass method (EMM), which usually establishes the connection between the local states and the structure of the energy spectrum. Therefore only qualitative considerations can be invoked to treat this behavior.

First, it is known that in the case of band degeneracy the mass of one or two branches of the spectrum is usually large (e.g., heavy holes). This seems to promote self-trapping. Second, band degeneracy is usually the result of degeneracy of the corresponding atomic states (e.g., p -type or sp -hybrid states), which form valence bonds. For example, ST of a hole in an alkali-halide crystal (V_k centers) is a quasimolecule of the Cl_2^{-1} type, bound by valence forces.³

In contrast to the ST states,^{4,5} the ST barrier^{5,6} that separates the free and ST states can have a spatial dimension $r_w \gg d$.⁷ The condition for this is satisfaction of the criterion $E_b \ll E_{FC}$, where E_b is the half-width of the band from which the self-trapping stems and E_{FC} is the Franck-Condon energy of the lattice deformation in the ST state.

It appears that the experimental data indicate that this criterion is satisfied in certain noble-gas crystals.⁸ If $r_w \gg d$, the ST barrier can be described on the basis of a continual model, i.e., in the EMM approximation. It is then possible to find its height W , shape, and also tunnel penetrability.⁹ These are important data, since the surmounting of the ST barrier usually controls the rate of the self-trapping.

We construct below the theory of a barrier for ST from a degenerate band with angular momentum ("spin") $S = 1$.

The most substantial result here is the spontaneous (Jahn-Teller) breaking of the ST barrier symmetry,^{6,10} which lowers the barrier. We investigate the dependence of W and of the barrier-anisotropy parameter A that characterizes the degree of symmetry breaking on the effective masses, deformation potentials, and elastic moduli. A similar analysis was carried out also for the ground state of a large-radius polaron—the only system that has a three-dimensional spectrum, is describable within the framework of the EMM, and has no ST barrier.¹¹

We consider in the present article crystals having cubic symmetry and confine ourselves to the case of a triply degenerate band. It includes holes in the absence of spin-orbit interaction, and Frenkel excitons. To simplify the calculations, which are cumbersome enough anyway, we retain in the Hamiltonian only spherical invariants and leave out the cubic, i.e., we neglect the corrugation of the bands. The angular momentum corresponding to the edge of the band is formally regarded as the spin $S = 1$ of the corresponding quasiparticle.

We investigate here, for the first time ever to our knowledge, a three-component nonlinear Schrödinger equation with allowance for integral nonlinear terms (preliminary data were reported in Ref. 10). The results of this investigation are applicable not only to ST in crystals, but also to a number of other physical problems. In the concluding section of the article we discuss briefly applications to the Urbach rule, to the theory of fluctuation tails of the density of states, to the theory of phase transitions (nonsphericity of the nuclei in systems with multicomponent order parameter), and others.

2. HAMILTONIAN AND WAVE FUNCTIONS. SYMMETRY BREAKING

We consider the problem of the ST barrier. In this case the total energy of a particle with spin $S = 1$ (hole, exciton) interacting with acoustic phonons through a deformation potential takes in the adiabatic approximation the form

$$H[\Psi, u] = H_k + H_{res} + H_{int} + H_{ph}, \quad (1)$$

where

$$H_k = \frac{1}{2m_l} \int |\operatorname{div} \Psi|^2 d^3r + \frac{1}{2m_t} \int |\operatorname{rot} \Psi|^2 d^3r \quad (2)$$

is the kinetic energy of the particle, the masses m_l and m_t correspond to the longitudinal and transverse spectrum branches,

$$H_{res} = \frac{\Delta_{lt}}{4\pi} \iint \frac{\operatorname{div} \Psi^*(\mathbf{r}) \operatorname{div} \Psi(\mathbf{r}')}{|\mathbf{r}-\mathbf{r}'|} d^3r d^3r' \quad (3)$$

is the resonant contribution to the energy and exists only for excitons that correspond to dipole-allowed transitions, Δ_{lt} is the longitudinal-transverse splitting,

$$H_{int} = (\alpha - \beta) \int |\Psi|^2 \operatorname{div} \mathbf{u} d^3r + \frac{3}{2} \beta \int \{(\Psi^* (\Psi \nabla) \mathbf{u} + \text{c.c.})\} d^3r \quad (4)$$

is the Hamiltonian of the interaction of the particle with the phonons, while α and β are the deformation potentials.¹² The term proportional to α in (4) corresponds to hydrostatic compression, and the term proportional to β to volume-conserving strains with zero trace:

$$H_{ph} = \int \left\{ \frac{2\mu + \lambda}{2} (\operatorname{div} \mathbf{u})^2 + \frac{\mu}{2} (\operatorname{rot} \mathbf{u})^2 \right\} d^3r \quad (5)$$

is the energy of the elastic deformation of the crystal, and λ and μ are Lamé coefficients.

The surface of the adiabatic potential $H[\mathbf{u}] = H[\Psi[\mathbf{u}], \mathbf{u}]$ is obtained from the condition

$$\delta H[\Psi, \mathbf{u}] / \delta \Psi^*(\mathbf{r}) = 0, \quad \int |\Psi(\mathbf{r})|^2 d^3r = 1, \quad (6)$$

which determines the $\Psi = \Psi[\mathbf{u}]$ dependence. We are interested in a stationary point of this surface—the lower saddle that separates the free and ST states. The equation that defines this point is

$$\delta H[\Psi[\mathbf{u}], \mathbf{u}] / \delta \mathbf{u}(\mathbf{r}) = 0. \quad (7)$$

Substituting expressions (1)–(5) in (6) and (7) we get

$$\begin{aligned} & -\frac{1}{2m_l} \operatorname{grad} \operatorname{div} \Psi + \frac{1}{2m_t} \operatorname{rot} \operatorname{rot} \Psi \\ & - \frac{\Delta_{lt}}{4\pi} \operatorname{grad} \operatorname{div} \int \frac{\Psi(\mathbf{r}')}{|\mathbf{r}-\mathbf{r}'|} d^3r' \\ & + (\alpha - \beta) \Psi \operatorname{div} \mathbf{u} + \frac{3}{2} \beta \{ \Psi \times \operatorname{rot} \mathbf{u} + 2(\Psi \nabla) \mathbf{u} \} = E \Psi, \quad (8) \\ & - (2\mu + \lambda) \operatorname{grad} \operatorname{div} \mathbf{u} + \mu \operatorname{rot} \operatorname{rot} \mathbf{u} = \mathbf{B}(\mathbf{r}), \quad (9) \end{aligned}$$

where

$$\mathbf{B}(\mathbf{r}) = (\alpha - \beta) \operatorname{grad} |\Psi|^2 + \frac{3}{2} \beta \{ \Psi \operatorname{div} \Psi^* + (\Psi^* \nabla) \Psi + \text{c.c.} \}. \quad (10)$$

Equation (9) is solved by transforming to the \mathbf{k} -representation

$$\mathbf{u}(\mathbf{k}) = \int \mathbf{u}(\mathbf{r}) \exp(-i\mathbf{k}\mathbf{r}) d^3r,$$

and similarly for $\mathbf{B}(\mathbf{k})$. It follows then from (9) that

$$\mathbf{u}(\mathbf{k}) = \left\{ \mathbf{B}(\mathbf{k}) - \frac{\mu + \lambda}{2\mu + \lambda} \frac{\mathbf{k}(\mathbf{k}\mathbf{B})}{k^2} \right\} \frac{1}{\mu k^2}. \quad (11)$$

In view of the unwieldy solution of (11), we assume for the preliminary analysis of the problem that $\beta = 0$. In this case we get from (11)

$$\mathbf{u}(\mathbf{r}) = \frac{\alpha}{4\pi(2\mu + \lambda)} \operatorname{grad} \int \frac{|\Psi(\mathbf{r}')|^2}{|\mathbf{r}-\mathbf{r}'|} d^3r' \quad (12)$$

and (8) takes the form

$$\begin{aligned} & -\frac{1}{2m_l} \operatorname{grad} \operatorname{div} \Psi + \frac{1}{2m_t} \operatorname{rot} \operatorname{rot} \Psi \\ & - \frac{\Delta_{lt}}{4\pi} \operatorname{grad} \operatorname{div} \int \frac{\Psi(\mathbf{r}')}{|\mathbf{r}-\mathbf{r}'|} d^3r' - \frac{\alpha^2}{2\mu + \lambda} |\Psi(\mathbf{r})|^2 \Psi = E \Psi(\mathbf{r}). \quad (13) \end{aligned}$$

When $\beta \neq 0$, the last term of the right-hand side of (13) is replaced by an integro-differential expression that is cubic in Ψ .

Since the variations with respect to \mathbf{u} and Ψ commute,¹¹ the problem of finding the lowest saddle W of the functional $H[\mathbf{u}]$ is equivalent to finding W for the functional, $\mathcal{J}[\Psi] = H[\Psi, \mathbf{u}[\Psi]]$ with \mathbf{u} defined by Eq. (11):

$$\begin{aligned} \mathcal{J}[\Psi] &= \frac{1}{2m_l} \int |\operatorname{div} \Psi|^2 d^3r + \frac{1}{2m_t} \int |\operatorname{rot} \Psi|^2 d^3r \\ &+ \frac{\Delta_{lt}}{4\pi} \iint \frac{\operatorname{div} \Psi^*(\mathbf{r}) \operatorname{div} \Psi(\mathbf{r}')}{|\mathbf{r}-\mathbf{r}'|} d^3r d^3r' \\ &- \frac{\alpha^2}{2(2\mu + \lambda)} \int |\Psi(\mathbf{r})|^4 d^3r. \quad (14) \end{aligned}$$

To determine to which eigenvalue E of Eq. (13) the lowest saddle point corresponds, we write down the virial theorem for the functional $\mathcal{J}[\Psi]$. This theorem, as usual, can be established by carrying out in \mathcal{J} the gauge transformation $\Psi(\mathbf{r}) = K^{3/2} \Psi(K\mathbf{r})$, differentiating with respect to K , and setting $K = 1$.^{11,6} At $\Delta_{lt} = 0$ we have

$$E = -\mathcal{J}[\Psi_{s.p.}] = -W. \quad (15)$$

It follows from (15) that the minimum W corresponds to the maximum eigenvalue of (13), or equivalently, to the negative eigenvalue with the smallest absolute value.

It is natural to assume, on the basis of the analogy with the theory of acceptor centers,^{12,13} that such an eigenvalue of the initial equation (8) is degenerate for a spherically-symmetric $\mathbf{u}(\mathbf{r})$, and the corresponding eigenfunctions belong to the angular momentum¹⁾ $J = S = 1$. This condition ensures the absence of nodes of the s -component, which usually makes the main contribution to the wave function Ψ . The degeneracy of the level E should lead, according to the Jahn-Teller theorem, to spontaneous breaking of the symmetry, since phonons with arbitrary symmetry are represented in the Hamiltonian H , particularly those belonging to the representation $\Gamma_{\psi_s} \otimes \Gamma_{\psi_s}$. We assume that the symmetry is lowered to the group $D_{\infty h}$. The triple degeneracy is then lifted, but certain connections between the eigenvector components remain and simplify the calculations that follow. The wave functions of the states obtained by splitting the term $J = 1$ take in the X, Y, Z basis the form

$$\Psi_0 = \begin{pmatrix} xzg \\ yzg \\ f \end{pmatrix}, \quad \Psi_{\pm 1} = \begin{pmatrix} 1 \\ \pm i \\ 0 \end{pmatrix} f + \begin{pmatrix} x \\ y \\ 0 \end{pmatrix} x_{\pm g} + \begin{pmatrix} 0 \\ 0 \\ 1 \end{pmatrix} x_{\pm zh}, \quad (16)$$

$$x_{\pm} = x \pm iy.$$

The subscript of Ψ_M is the projection of the angular momentum on the symmetry axis z . The functions f, g , and h are real and depend only on $\rho^2 = x^2 + y^2$ and z^2 . The question of further symmetry lowering that lifts the degeneracy of the states $\Psi_{\pm 1}$ is discussed below.

We can now establish certain singularities in the behavior of the functions Ψ_0 and $\Psi_{\pm 1}$. If we substitute them in (13) we see that the asymptotic form of Ψ as $r \rightarrow \infty$ is determined by the third term. For example, for Ψ_0 as $r \rightarrow \infty$ we have

$$-\frac{1}{4\pi} \Delta_{it} \text{grad div} \begin{pmatrix} 0 \\ 0 \\ f_0/r \end{pmatrix} \approx E \Psi_0, \quad f_0 \equiv \int f(\rho, z^2) d^3r. \quad (17)$$

It follows from (17) that asymptotically we have

$$\Psi_0 \propto r^{-5} \begin{pmatrix} 3xz \\ 3yz \\ 3z^2 - r^2 \end{pmatrix}, \quad (18)$$

with $\Psi_{\pm 1}$ similar. The asymptotic form $\propto r^{-3}$ describes a dipole-dipole mechanism of exciton motion.

A similar asymptotic form appears also at $\Delta_{it} = 0$, if $\tilde{\mu}^{-1} \equiv m_l/m_t \rightarrow 0$. The inequality $\tilde{\mu} \gg 1$ corresponds to the usual situation when (longitudinal) holes with helicity $\nu = 0$ and mass m_l are light, and the (transverse) holes with $\nu = \pm 1$ and mass m_t are heavy.²⁾ In the limit as $\tilde{\mu} \rightarrow \infty$ we must put $\text{div } \Psi = 0$ (Ref. 15) and to ensure a transverse character of Ψ we must retain in the nonlinear term of (13) only the transverse part. Then (13) takes the form

$$-\frac{1}{2m_t} \Delta \Psi - \frac{1}{4\pi} \frac{a^2}{2\mu + \lambda} \text{rot rot} \int \frac{|\Psi(\mathbf{r}')|^2 \Psi(\mathbf{r}')}{|\mathbf{r} - \mathbf{r}'|} d^3r' = E \Psi(\mathbf{r}). \quad (19)$$

With a transformation exactly the same as in the derivation of (17) we arrive again to Eq. (18). At finite $\tilde{\mu} \gg 1$ the relation $\propto r^{-3}$ is an intermediate asymptotic form (in analogy with the acceptor wave function.¹⁶⁾

The system (8)–(9) cannot be solved analytically, and numerical methods were used. The vector Ψ was chosen in the form (16) with allowance for the possibility of its slow asymptotic decrease (17). To determine $\mathbf{u}(\mathbf{r})$ it is convenient to take first the curl of both sides of (9). Then

$$\mu \text{rot } \Delta \mathbf{u}(\mathbf{r}) = -\text{rot } \mathbf{B}(\mathbf{r}). \quad (20)$$

Single integration of (20) leads to

$$\mu \Delta \mathbf{u} = -\mathbf{B} + \nabla \chi(\rho, z^2), \quad (21)$$

where χ is an arbitrary function of ρ and z^2 . The solution of (21) is

$$\mathbf{u}(\mathbf{r}) = -\frac{1}{4\pi\mu} \int \frac{-\mathbf{B} + \nabla \chi}{|\mathbf{r} - \mathbf{r}'|} d^3r'. \quad (22)$$

It follows from (21) that $\mathbf{u}(\mathbf{r})$ has the form

$$\mathbf{u}(\mathbf{r}) = \begin{pmatrix} xp(\rho, z^2) \\ yp(\rho, z^2) \\ zq(\rho, z^2) \end{pmatrix}. \quad (23)$$

It is easy to determine from (22) the asymptotic behavior of $\mathbf{u}(\mathbf{r})$ as $r \rightarrow \infty$. Assuming that χ falls off rapidly enough to

ensure convergence of the integral in (22) and recognizing that $\mathbf{B}(\mathbf{r})$ has the same symmetry structure as $\mathbf{u}(\mathbf{r})$ [see (23)] we find that $\mathbf{u}(\mathbf{r}) \propto r^{-2}$ as $r \rightarrow \infty$.

In the numerical solution, Ψ and \mathbf{u} were expanded in the basis functions $C_n^l z^n (r^2 + c^2)^{-1/2}$. The integers n and l were chosen such that as $r \rightarrow \infty$ the functions Ψ and \mathbf{u} decreased no more slowly than r^{-3} and r^{-2} , respectively, and had the correct behavior as $r \rightarrow 0$. The number of parameters C_n^l reached 25. After solving the nonlinear system of equations for C_n^l , which determines the absolute minimum of the functional H when c is given, we minimized the solution with respect to c : $W = \max H(c)$. It corresponds to the lowest saddle point.

3. HEIGHT AND SHAPE OF ST BARRIER

In this section we report the results of the calculation of the height of the ST barrier. We begin with the simplest case $b = \Delta_{it} = 0$. Equation (8) and (9) are then satisfied at

$$\text{rot } \mathbf{u} = 0, \quad a |\Psi|^2 + (2\mu + \lambda) \text{div } \mathbf{u} = 0.$$

After eliminating \mathbf{u} , the wave function Ψ is given by the equation

$$-\frac{1}{2m_t} \text{grad div } \Psi + \frac{1}{2m_t} \text{rot rot } \Psi - \frac{a^2}{2\mu + \lambda} |\Psi|^2 \Psi = E \Psi. \quad (24)$$

At $m_l = m_t \equiv m_h$ (here and below m_h is the heavy mass) the first two terms are gathered into $-\Delta \Psi / 2m_h$ and (24) breaks up into three identical scalar equations:

$$-\frac{1}{2m_h} \Delta \Psi - \frac{a^2}{2\mu + \lambda} |\Psi|^2 \Psi = E \Psi. \quad (25)$$

Equation (25) has an eigenvalue corresponding to nodeless Ψ :

$$E = -W_{sc} \approx -44 \frac{(2\mu + \lambda)^2}{m_h^3 a^4}. \quad (26)$$

The barrier height will hereafter be given in units of W_{sc} :

$$w_M(\tilde{\mu}) = W_M(\tilde{\mu}) / W_{sc}.$$

Figure 1a shows a plot of $w_M(\tilde{\mu})$. It can be seen that the $w_0(\tilde{\mu})$ curve always passes lower than $w_{\pm 1}(\tilde{\mu})$; the curves meet only at $\tilde{\mu} = 1$. Figure 1b shows the anisotropy coefficient $A(\tilde{\mu})$ defined as

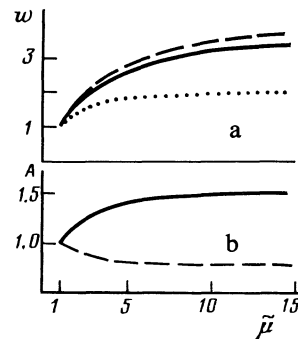


FIG. 1. Height w of ST barrier (a) and anisotropy coefficient A (b) as functions of $\tilde{\mu}$. The solid and dashed curves are for $M = 0$ and ± 1 , respectively. Dotted— $|E'_{\pm 1}(\mu)|/W_{sc}$.

$$A(\tilde{\mu}) = z_{1/2}(\tilde{\mu})/\rho_{1/2}(\tilde{\mu}),$$

where $z_{1/2}$ and $\rho_{1/2}$ are the semi-axes of the surface $|\Psi(\mathbf{r})|^2 = |\Psi(0)|^2/2$. It can be seen from Fig. 1b that $|\Psi(\mathbf{r})|^2$, and hence also the deformation (i.e., $\text{div } \mathbf{u}$) are prolate along z axis in the state $M = 0$ and oblate in the state $M = \pm 1$. The deviation of A_M from unity is the main indicator of the degree of symmetry breaking; it can be seen that at $\tilde{\mu} \gg 5$ the coefficient A reaches values ≈ 1.5 and 0.8 for $M = 0$ and 1 , respectively. At $\tilde{\mu} < 1$ the states with $M = 0$ become oblate, and those with $M = \pm 1$ prolate. The surfaces $|\Psi(\mathbf{r})|^2$ can have complicated shapes. We shall not describe them here; they are outlined for the limiting case $\tilde{\mu} \rightarrow 0$ in Fig. 1 of Ref. 14.

It can be seen from Fig. 1a that in the range of $\tilde{\mu}$ from 1 to infinity the value of w_0 increases by a numerical factor ≈ 4 . The limiting barrier height is then $W(\infty) \equiv W(\tilde{\mu} = \infty)$, i.e., it corresponds to $m_l = 0$ and $m_l = m_h$:

$$W_0(\infty) \approx 162(2\mu + \lambda)^2/m_h^3 a^4. \quad (27)$$

A measure of the symmetry breaking in the state $M = 0$ can be, besides A_0 , also the difference between the energies of the states $M = 0$ and ± 1 (E'_0 and $E'_{\pm 1}$) in the deformation field corresponding to Ψ_0 . According to (15), in this field the energy is $|E'_0| = |E_0| = W_0(\tilde{\mu})$. At arbitrary spherical-symmetry deformation $E'_0 = E'_{\pm 1}$. It can be seen from Fig. 1a that $|E'_{\pm 1}(\tilde{\mu})|$ deviates substantially from $W_0(\tilde{\mu})$.

It is important to estimate the barrier-height change due to the choice of the degenerate solutions (16) subjected to the Jahn-Teller effect. For this purpose it is necessary to compare the W_0 obtained above for the "vector" states (with initial angular momentum $J = 1$) with the barrier height $W(J = 0)$ for spherically symmetric states with total angular momentum $J = 0$. In this case $\Psi(\mathbf{r}) = \text{rg}(r)$. For these $\text{curl } \Psi = 0$, and according to (8) the Schrödinger equation contains only the mass m_l of the light holes. From this, taking (27) into account, it follows that $W(J = 0)/W_0 \sim \tilde{\mu}^3$. Therefore at $\tilde{\mu} \gg 1$ the choice of the "vector" solution decreases W in order of magnitude, since the scales $W(J = 0)$ and W_0 are determined by different masses, m_l and m_h , respectively.

The states with $M = \pm 1$ are degenerate, and this degeneracy should be lifted by the nonaxially symmetric deformations. Calculations for such deformations are extremely complicated, and we do not present them here. They are furthermore apparently unnecessary. Indeed, since $w_{\pm 1}(\tilde{\mu}) > w_0(\tilde{\mu})$ in the entire region $\tilde{\mu} > 1$, it is natural to propose that in the course of the decay of the states with $M = \pm 1$ the system goes through nonaxially symmetric states and assumes in final analysis to a form corresponding to $M = 0$, but with a different direction of the symmetry axis.

An important factor is how steeply the surface of the adiabatic potential, i.e., of the functional $H[\mathbf{u}]$, rises near the saddle W_0 . It can be assumed that the rise is least steep where the $W_0(\tilde{\mu})$ and $W_{\pm 1}(\tilde{\mu})$ curves are close to each other. This takes place, in particular, at $\tilde{b} = \Delta_{ll} = 0$. The lowest saddle W_{spher} of the functional $H[\mathbf{u}]$, considered in the class of spherically symmetric deformations $\text{div } \mathbf{u}(\mathbf{r})$, was also calculated for this case,¹⁷ and was found to exceed $W_{\pm 1}$ only

slightly. Thus, at any rate when $\tilde{b} = \Delta_{ll} = 0$, the system can surmount with comparable probability the ST barrier while in essentially different configurations.

There is a special case when the decisive role can be played by states with $M = \pm 1$. It should be realized in hexagonal and tetragonal crystals, in which the crystal splitting of the band with $J = 1$ causes the top of the doubly degenerate valence band (with symmetry x, y) to lie above the top of the nondegenerate band (with symmetry z). Let this splitting be $\Delta_{cr} \gg W$, but nonetheless shorter than the distance to the other band. The z -band can then be excluded from consideration, and the EMM Hamiltonian can be expressed in the quasi-spherical approximation in terms of the masses m_l and m_t in (2):

$$H_k = -\frac{1}{4} \left(\frac{1}{m_l} + \frac{1}{m_t} \right) (\partial_{xx} + \partial_{yy}) - \frac{1}{2m_t} \partial_{zz} - \frac{1}{4} \left(\frac{1}{m_l} - \frac{1}{m_t} \right) \times \left\| \begin{array}{cc} \partial_{xx} - \partial_{yy} & 2\partial_{xy} \\ 2\partial_{xy} & \partial_{yy} - \partial_{xx} \end{array} \right\|. \quad (28)$$

Here $\partial_{xy} \equiv \partial^2/\partial x \partial y$, and similarly for the other derivatives. For such H_k in an equation similar to (8), the axial symmetry is spontaneously broken, i.e., the symmetry in the xy plane is lowered. A calculation for the case $\tilde{b} = \Delta_{ll} = 0$ with a three-parameter Gaussian function Ψ :

$$\Psi_x = \Psi_y = 0, \quad \Psi_z \propto \exp \left\{ - \left(\frac{x^2}{c_x^2} + \frac{y^2}{c_y^2} + \frac{z^2}{c_z^2} \right) \right\},$$

leads to the following expressions for W and A :

$$A = \frac{c_x}{c_y} = \frac{m_t}{m_l}, \quad W = 2\pi^3 \frac{(2\mu + \lambda)^2}{m_l^2 m_t a^4}. \quad (29)$$

Figure 2 shows the dependences of w and A on the ratio of the deformation potentials $\beta = \tilde{b}/a$ at three values of $\tilde{\mu}$ and two values of the Poisson constant $\sigma = \lambda/2(\lambda + \mu)$. It can be seen from Fig. 2 that the difference between w_0 and $w_{\pm 1}$ increases on the whole, and furthermore quite appreciably, when β increases. It is very important that $w_0 < w_{\pm 1}$ in the entire range of the parameter values. This agrees with the assumption made above that the lowest barrier corresponds to $M = 0$. It can also be seen from Fig. 2 that the change of σ does not influence qualitatively the course of the curves. On the contrary, the dependence on β is strong. Application of the potential \tilde{b} can lower considerably the barrier, which has in all cases a maximum near $\tilde{b} = 0$.

Particularly noteworthy are the $A(\beta)$ curves with $\tilde{\mu} = 1$, for in this case the symmetry breaking is exclusively due to $\beta \neq 0$. A goes through unity when $\tilde{b} = 0$. The states are oblate at $\beta < 0$ and prolate at $\beta > 0$. The unique connection noted above between the signs of $(A - 1)$ and $(\tilde{\mu} - 1)$ is absent at $\tilde{b} \neq 0$. It is restored, however, with increasing $\tilde{\mu}$.

We proceed now to the case $\Delta_{ll} \neq 0$, which is important for excitons, and put $\tilde{b} = 0$. The exciton energy spectrum is shown in Fig. 3. the dependence of w on $\delta = \Delta_{ll}/W_{sc}$ is shown in Fig. 4. Curve 1 corresponds to $\tilde{\mu} = 1$, $\tilde{b} = 0$, i.e., to a situation wherein the symmetry breaking is due exclusively to $\delta \neq 0$ —to the dipole-dipole interaction. As $\delta \rightarrow \infty$ both w and A assume the same asymptotic forms as at $\tilde{\mu} \rightarrow \infty$. The reason is that in both limiting cases the contribution of the longitudinal excitons is fully suppressed. In particular, Eq.

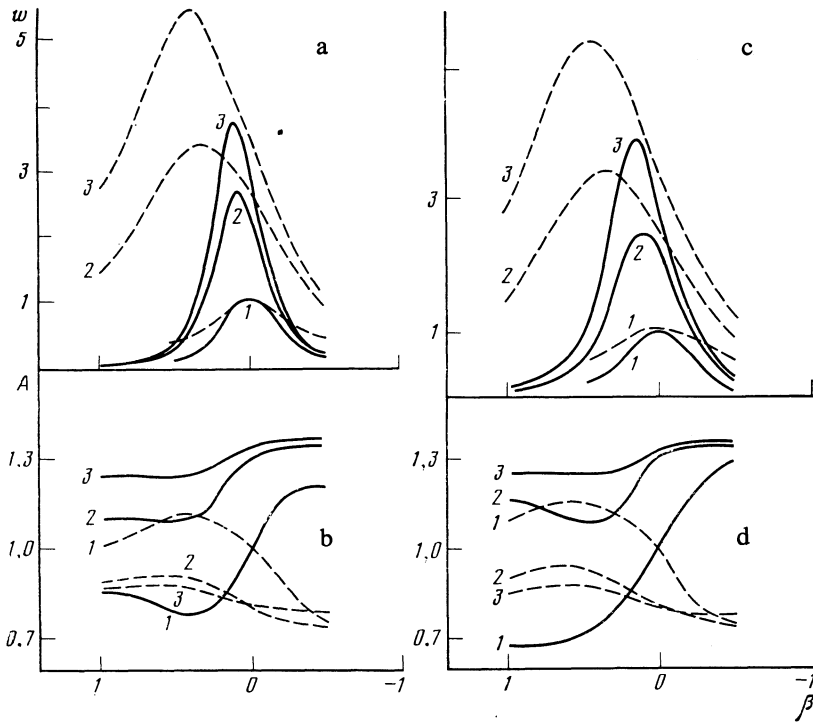


FIG. 2. Dependence of the height w of the ST barrier (a, c) and of the anisotropy coefficient A (b, d) on β at $\Delta_{tt} = 0$. The solid and dashed curves are for $M = 0$ and $M = \pm 1$; curves 1— $\tilde{\mu} = 1$, 2— $\tilde{\mu} = 4$, 3— $\tilde{\mu} = 10$. Figs a and b are for $\sigma = 0.35$, while c and d are for $\sigma = 0.15$.

(27) is valid both for $\tilde{\mu} \rightarrow \infty$ and arbitrary δ , and for $\delta \rightarrow \infty$ and arbitrary $\tilde{\mu}$. It can be seen from Fig. 4, however, that the monotonic increase of w as a function of δ , which is initially relatively rapid, becomes later quite slow, at a scale $\delta \sim 10^2$.

4. POLARONS

Polarons in crystals with degenerate band structures were considered hitherto only in the weak coupling approximation.^{18,19} We consider below the case of the adiabatic limit. The functional of the total polaron energy H , just as in Ref. 11, consists of the kinetic energy (2), of the interaction energy

$$H_{int} = e \int |\Psi(\mathbf{r})|^2 \varphi(\mathbf{r}) d^3r \quad (30)$$

and of the energy of polarization of the medium

$$H_{ph} = \frac{1}{8\pi\epsilon} \int (\nabla\varphi)^2 d^3r, \quad (31)$$

where $\epsilon^{-1} = \epsilon_\infty^{-1} - \epsilon_0^{-1}$, while ϵ_0 and ϵ_∞ are the low- and high-frequency dielectric constants.

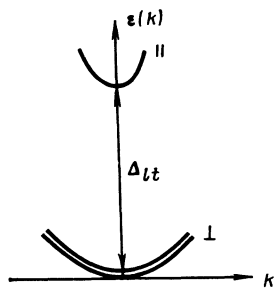


FIG. 3. Energy spectrum of exciton with account taken of the splitting Δ_{tt} . The doubly degenerate band of the transverse excitons is shown symbolically by a double line.

The wave function Ψ , just as in the ST barrier problem, is a three-component vector, and the problem is solved in analogy with the procedure described at the end of Sec. 2, except that the vector field $\mathbf{u}(\mathbf{r})$ that decreases asymptotically like r^{-2} is replaced by a scalar field $\varphi(\mathbf{r})$ that decreases like r^{-1} . The results of the calculations for $M = 0$ are shown in Fig. 5. Comparison with Fig. 1 shows that the dependence of the parameters on $\tilde{\mu}$ is noticeably weaker for a polaron than for the ST barrier; in particular, the polaron anisotropy is relatively small, $(A - 1) \lesssim 0.1$.

The very presence of the anisotropy of $\varphi(\mathbf{r})$, however, leads to qualitative changes in the spectrum of the polaron, since it acquires two rotational degrees of freedom—rotations about axes perpendicular to the symmetry axis. It is convenient to express all the parameters in term of the Fröhlich coupling constant $\alpha = (m_h e^4 / 2\omega_0 \epsilon^2)^{1/2}$, where ω_0 is the

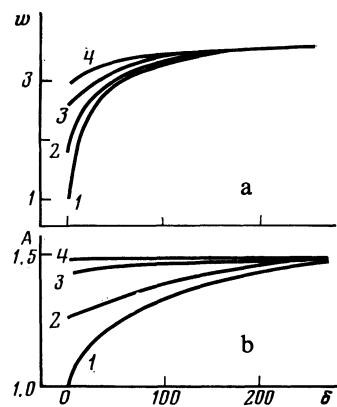


FIG. 4. Dependence of the height w of the ST barrier (a) and of the anisotropy A (b) on δ . Different curves correspond to different mass ratios: $\tilde{\mu}$: 1—1, 2—2, 3—5, 4—10.

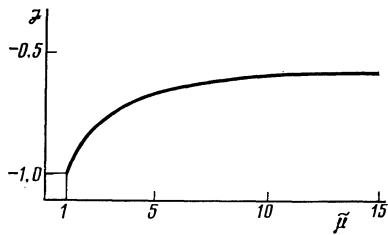


FIG. 5. Polaron energy \mathcal{J} as a function of $\tilde{\mu}$ ($M=0$) \mathcal{J} is expressed in units of $|\mathcal{J}_{sc}| = 0.0544 me^4/\epsilon^2$.

phonon frequency. The constant α is defined in terms of the heavy-hole mass m_h , since it is precisely this mass which determines the scales of the energy \mathcal{J} , of the effective mass m_p , and of the radius r_p of the polaron in the adiabatic limit ($\mathcal{J} \sim \alpha^2 \omega_0$, $m_p \sim \alpha^4 m_h$ and $r_p \sim (\alpha^2 m_h \omega_0)^{-1/2}$). For the rotational quantum we obtain then $\epsilon_r \sim I^{-1} \sim \omega_0/\alpha^2$, where $I \sim m_p r_p^2$ is the polaron moment of inertia. In the theory of the spherically symmetric polaron there have been investigated so far the contributions $\sim \alpha^2 \omega_0$ and $\sim \alpha^0 \omega_0$ to the energy. The last term consists of the Pekar contribution $-1.5\omega_0$, which is connected with the translational zero modes,¹¹ and an additional contribution due to the softening of the other vibrational modes near the polaron^{20,21}; the total coefficient of the later term is ≈ -2.836 .²¹ The axially symmetric polaron has five zero modes (three translational and two rotational), so that is clear beforehand that the coefficient of should not have a modulus larger than 2.5.

5. RELATED SYSTEMS

A number of systems are either directly physically related to the ST barrier in crystals and to the polaron, or are described by similar equations.

The analog of the ST barrier in crystals is the barrier that separates the homogeneous plasma state from the state with plasma cavitons.²² The existence of this ST barrier was demonstrated by us in Ref. 14; it is described by Eqs. (8) and (9) with $\tilde{b} = \Delta_{it} = 0$ in the limit as $\tilde{\mu} \rightarrow 0$. Analogs of the polaron are the fluctuons and phasons that can appear in various systems with diverse mechanisms of interaction between an electron and a medium.² The detailed mechanism of the interaction alters only the form of the nonlinear term in (13), but the entire physical picture remains unchanged: the only essential requirement for the onset of spontaneous symmetry lowering is that the electron band be degenerate.

In the Urbach-effect theory developed by Ioselevich²⁴ as applied to a Frenkel exciton, the determination of the absorption coefficient in the region of large energy deficits Δ reduces to solution of an equation analogous to (13). It was proposed in Ref. 24 that the exciton interacts with polar nondispersive optical phonons having a frequency ω_0 . The coefficient of the nonlinear term in (13) is then replaced by $2\nu E_{FC}$, where ν is the volume of the unit cell and E_{FC} is the deformation energy (see Sec. 1). The problem was solved in Ref. 24 in a scalar variant with $\Delta_{it} = 0$. Generalization to the case of a degenerate band is possible by direct use of the results of Sec. 3. It is necessary for this purpose to introduce

an equivalent mass $m_{eq}(\tilde{\mu})$, expressed in terms of the dimensionless height w of the ST barrier by means of the formula

$$m_{eq}(\tilde{\mu}) = m_i w^{-1/2}, \quad (32)$$

and replace the scalar mass in the equations of Ref. 24 by m_{eq} . The $w(\tilde{\mu})$ that enter here are shown by the solid curve in Fig. 1a. In particular, for limiting cases of high ($T \gg \omega_0$) and low ($T \ll \omega_0$) temperatures the absorption coefficient $\kappa(\Delta)$ is given by

$$\kappa \propto \exp\left(-\frac{2(W\Delta)^{1/2}}{T}\right), \quad \kappa \propto \exp\left(-\frac{4(W\Delta)^{1/2}}{\omega_0}\right). \quad (33)$$

Equations (33), which establish the direct connection between the absorption tails and the ST barrier, provide an independent method of measuring W .

Equations (13) with $\Delta_{it} = 0$ is also an equation for the level-density distribution near the band edge in a semiconductor within the framework of the optimal-fluctuation method; it is assumed that the random potential can be simulated by white noise. For a nondegenerate band this method was developed by Gal'perin and Lax,²⁵ by Zittarz and Langr,²⁶ and by Lifshitz.²⁷ The tails $\tilde{\rho}(E)$ of the density of state determine the density of the local levels in the forbidden band of a semiconductor and the carrier density in a zero-gap semiconductor at $T=0$.²⁸ For a nondegenerate band,

$$\tilde{\rho}(E) \propto \exp\{-\mathcal{C}(E)\}, \quad \mathcal{C}(E) \approx 13.3E^{1/2}/B_0 m^{3/2}, \quad (34)$$

B_0 is the white-noise constant. Of greatest physical importance are the $\tilde{\rho}(E)$ tails near the edge of a degenerate valence band, since the large effective mass of the heavy holes slows down the falloff of $\tilde{\rho}(E)$. It can be shown¹⁷ that for a nondegenerate spectrum Eq. (34) remains in force if m is replaced in it by m_{eq} , which is defined by (32). It is very important that for a degenerate band the optimal fluctuations are nonspherical. Permogorov *et al.*,²⁹ who observed the spectral dependence of the polarization coefficient of edge luminescence in $\text{CdS}_{1-x}\text{Se}_x$, suggested that it is connected with the nonsphericity of the fluctuations of the impurity locations.

6. ANISOTROPY OF PHASE-TRANSITION NUCLEI

In this section we draw an analogy between an ST barrier and formation of phase-transition nuclei. In first-order transitions near the lability point,³⁰ as well as in first-order transitions that are close to second-order ones, we can, in the spirit of the Landau theory³¹ expand the free energy F in terms of the order parameter. The equations that minimize the free energy are analogous to the equations of the self-trapping theory. The order parameter plays the role of the wave function Ψ , but unlike the latter there is no normalization condition, for it. For a multicomponent (say, vector or tensor) order parameter, the problem is mathematically equivalent to self-trapping from a degenerate band, and the role of the critical nucleus is played by the ST barrier. By analogy with Secs. 2 and 3 we can expect a nonspherical nucleus in the case of a multicomponent order parameter; this possibility will be demonstrated below.

Let, for example, the system be described by a complex order parameter $Q_{ij}(i, j = 1 \dots n)$. We write down a model

free-energy functional made up entirely of spherical invariants in the form

$$F[Q] = \int \{N_1 |\partial_\alpha Q_{ij}|^2 + N_2 \partial_\alpha Q_{ij}^* \partial_\beta Q_{mj} \hat{J}_{ii}^\alpha \hat{J}_{lm}^\beta + a(T - T_c) |Q_{ij}|^2 - 1/2 b (Q_{ij}^* Q_{ij})^2\} d^3r. \quad (35)$$

Here N_1 and N_2 as well as a and b are positive constant coefficients, T_c is the transition temperature, $\hat{J}^\alpha = \|\hat{J}_{ij}^\alpha\|$ are angular-momentum matrices corresponding to a representation with total angular momentum J ; repeated indices mean summation. We consider only the case $T > T_c$. The local minimum of F at the point $Q = 0$ corresponds to a metastable phase, the lower saddle point $F[Q_{s.p.}]$ corresponds to a critical nucleus, and $F[Q] < 0$ at large q corresponds to transition to a stable phase. The stationary points $F[Q]$ are defined by the nonlinear equation

$$-N_1 \Delta Q_{ij} - N_2 J_{ii}^\alpha J_{lm}^\beta \partial_{\alpha\beta} Q_{mj} - b (Q_{lm}^* Q_{lm}) Q_{ij} = -a(T - T_c) Q_{ij}. \quad (36)$$

The solution of (36) at the saddle point $F[Q]$ corresponds to the critical nucleus.

The transition to the analogous quantum-mechanical problem is by the transformation

$$Q_{ij} = \frac{1}{G} \left(\frac{N_1}{b} \right)^{1/2} \Psi_{ij}, \quad \mathbf{r} = \frac{b}{N_1} G \xi, \quad G = \int Q_{ij}^* Q_{ij} d^3r, \quad (37)$$

which ensures the normalization of Ψ and transforms (36) into

$$-\Delta \Psi_{ij} - (N_2/N_1) J_{ii}^\alpha J_{lm}^\beta \partial_{\alpha\beta} \Psi_{mj} - (\Psi_{lm}^* \Psi_{lm}) \Psi_{ij} = \varepsilon \Psi_{ij}, \quad \varepsilon = -ab^2 G^2 (T - T_c) / N_1^3, \quad (38)$$

which is analogous to (13). Here Ψ_{ij} is a multicomponent wave function and $\varepsilon = \varepsilon(N_2/N_1)$ is the eigenvalue of Eq. (38), i.e., the Lagrange multiplier connected with the parameters of the Hamiltonian (35) by the second equation of (38). The minimum work $R_{\min} = F_{s.p.}$ necessary to produce a critical nucleus is equal to the value of $F[\Psi]$ at the saddle point. Using the virial theorem with special account taken of the third term of (35), we can show that

$$R_{\min} = \frac{2}{b} N_1 (|\varepsilon| a N_1)^{1/2} (T - T_c)^{1/2}. \quad (39)$$

Equation (39) generalizes the known result³¹ of the van der Waals theory of the critical point. The radius r_{cr} of the critical nucleus at $N_1 \sim N_2 \sim N$ is

$$r_{cr} \sim [N/a(T - T_c)]^{1/2}. \quad (40)$$

According to the Arrhenius law, the probability of classical nucleus formation is $\propto \exp(-R_{\min}/T)$. (Ref. 31).

Equation (30) was investigated for three- and four-component wave functions in Refs. 10, 14, 17 and 32, and in the preceding sections of the present paper. Common to these equations is spontaneous symmetry breaking. It is experienced by the form factor $Q_{ij}^*(\mathbf{r})Q_{ij}(\mathbf{r})$ of the nucleus. The anisotropy of the nucleus depends on the ratio N_2/N_1 (for an example see Fig. 1b). At $N_2 = 0$ the anisotropy vanishes. Thus, for systems described by multicomponent order parameters, the nuclei as a rule are not spherical and are, for example, cigar- or disk-shaped.³⁾

7. CONCLUSION

We investigated spontaneous symmetry breaking in an ST barrier and in a strong-coupling polaron in crystals with degenerate bands with spin $S = 1$. The parameters that determine the degree of symmetry breaking are the ratio $\bar{\mu}$ of the heavy and light masses, as well as the parameters of the interaction of the particle (hole, exciton) with the medium. We have shown that in most cases the states are prolate at $\bar{\mu} > 1$. However, the shape of the $|\Psi(\mathbf{r})|^2$ cloud is substantially influenced also by other parameters of the Hamiltonian. In particular, it may turn out to be oblate at a definite ratio of the deformation potentials, if $\bar{\mu}$ is not too large in this case. The scale of the energy and spatial parameters of the polaron and of the ST barrier is determined by the heavy mass. As applied to the polaron, it leads to an increase of the coupling constant α and produces by the same token more favorable conditions for the onset of strong-coupling polarons.

The conclusions concerning the shape of the ST barrier can apparently hold also for noble-gas crystals, in most of which the existence of quasimolecular ST excitons (m -excitons) of the R^* type can be reliably established. The conclusion that the ST barrier is prolate indicates that the asymmetric form of the ST state is formed already during the stage of surmounting the ST barrier. With the ST states so formed, there is no need for the intermediate self-trapping stage, namely passage through symmetric quasi-atomic states (a -excitons), as is frequently proposed in the interpretation of the experimental data. Suemoto and Kanzaki³⁴ have shown convincingly that in Ne, where a - and m -excitons exist, the former can be transformed into the latter by a photochemical reaction. The need for photochemical activation points to the presence of a barrier between the a - and m -states. At the same time, their data (Ref. 34, Fig. 1) show that at short times ($\sim 0.2 \mu\text{sec}$) after the pulse that produces the excitons, the emission of the m -excitons is noticeably more intense than that of the a -excitons. This agrees with the conclusions of Sec. 3 concerning the maximum rate of self-trapping from a band state via states of lowered symmetry.

Analogous arguments apply also to ST by quasimolecular holes, if the main contribution to their formation is made by a nonpolar interaction.

The calculations were performed in the spherical model. Obviously, inclusion of cubic invariants in the Hamiltonian "ties" the symmetry axis of the self-trapped exciton or hole to one of the symmetric crystallographic directions. An attempt to take into account cubic invariants was made in Ref. 35. There, however, several spherical invariants were left out and, in particular, a scalar mass was used. As a result, the basic manifestation of the Jahn-Teller effect, namely the nonsphericity of $|\Psi(\mathbf{r})|^2$, is missing from Ref. 35.

Many of the foregoing results can be generalized to apply to other systems. Above all, polaron and ST-barrier symmetry breaking occurs also at a spin $S = 3/2$ (Ref. 10). A number of other examples were dealt with in Secs. 5 and 6.

We are grateful to A. S. Ioselevich, V. I. Mel'nikov, and S. V. Meshkov for numerous helpful discussions.

¹⁾This assumption is confirmed by the results of Sec. 3.

²⁾The inverse limiting case $\bar{\mu} \ll 1$ is realized in a plasma for electromagnetic

and plasma waves. It is considered in Ref. 14.

³We are grateful to G. E. Volovik for pointing out to us that the conclusion that the nucleus is not spherical can apply also to nucleus formation in a transition between the *A* and *B* phases of ³He, a problem so far unsolved.³³

¹C. Kittel, Introduction to Solid State Physics, 4th ed., Wiley, 1971.

²Ch. B. Lushchik, in: Excitons, E. I. Rashba and M. D. Sturge, eds., North Holland, 1982, p. 505.

³T. G. Kastner and W. J. Kanzig, J. Phys. Chem. Solids **3**, 178 (1957).

⁴M. F. Deigen and S. I. Pekar, Zh. Eksp. Teor. Fiz. **21**, 803 (1951). Y. Toyozawa, Progr. Theor. Phys. **26**, 29 (1961).

⁵E. I. Rashba, Opt. Spektrosk. **2**, 77 (1957).

⁶E. I. Rashba, Ref. 2, p. 543.

⁷E. I. Rashba, Fiz. Nizk. Temp. **3**, 524 (1977) [Sov. J. Low Temp. Phys. **3**, 254 (1977)].

⁸I. Fugol, Adv. Phys. **27**, 1 (1978).

⁹S. V. Iordanskii and E. I. Rashba, Zh. Eksp. Teor. Fiz. **74**, 1872 (1978) [Sov. Phys. JETP **47**, 975 (1978)].

¹⁰F. V. Kusmartsev and E. I. Rashba, Pis'ma Zh. Eksp. Teor. Fiz. **33**, 164 (1981) [JETP Lett. **33**, 158 (1981)]. In the book. Group-Theoretical Methods in Physics, [in Russian] Nauka, 1983, Vol. II, p. 453.

¹¹S. I. Pekar, Research in Electron Theory of Metals, US AEC Transl. AEC-tr-555 (1963).

¹²G. L. Bir and G. E. Pkus, Symmetry and Strain-Induced Effects in Semiconductors, Wiley, 1975.

¹³W. Kohn, Solid State Physics, F. Seitz and D. Turbull, eds., Vol. 5 p. 256, 1957.

¹⁴F. V. Kusmartsev and E. I. Rashba, Zh. Eksp. Teor. Fiz. **84**, 2064 (1983) [Sov. Phys. JETP **57**, 1202 (1983)].

¹⁵L. V. Keldysh, *ibid.* **45**, 364 (1963) [**18**, 253 (1964)].

¹⁶B. L. Gel'mont and M. I. D'yakonov, *ibid.* **62**, 713 (1972) [**35**, 377 (1972)].

¹⁷F. V. Kusmartsev and E. I. Rashba, Pis'ma Zh. Eksp. Teor. Fiz. **37**, 106 (1972) [JETP Lett. **37**, 130 (1983)].

¹⁸H. R. Trebin and U. Rosler, Phys. State. Sol. (b) **70**, 717 (1975).

¹⁹G. Beni and T. M. Rice, Phys. Rev. **B15**, 840 (1977).

²⁰V. I. Mel'nikov and E. I. Rashba, Pis'ma Zh. Eksp. Teor. Fiz. **10**, 95, 359 (1969) [JETP Lett. **10**, 60, 228 (1969)].

²¹S. J. Miyake, J. Phys. Soc. Jpn. **41**, 747 (1976).

²²V. E. Zakharov, Zh. Eksp. Teor. Fiz. **62**, 1745 (1972) [Sov. Phys. JETP **35**, 908 (1972)].

²³M. A. Krivoglaz, Usp. Fiz. Nauk **111**, 617 (1973) [Sov. Phys. Usp. **16**, 856 (1974)].

²⁴A. S. Ioselevich, Zh. Eksp. Teor. Fiz. **83**, 743 (1982) [Sov. Phys. JETP **56**, 415 (1982)].

²⁵B. I. Halperin and M. Lax, Phys. Rev. **148**, 722 (1966).

²⁶J. Zittarz and J. S. Langer, Phys. Rev. **184**, 741 (1966).

²⁷I. M. Lifshitz, Zh. Eksp. Teor. Fiz. **53**, 743 (1967) [Sov. Phys. JETP **26**, 462 (1968)].

²⁸N. N. Ablyazov, M. E. Raikh, and A. L. Efros, Pis'ma Zh. Eksp. Teor. Fiz. **38**, 103 (1983) [JETP Lett. **38**, 120 (1983)].

²⁹S. A. Permogorov, A. N. Reznitskii, S. Yu. Verbin, and V. G. Lysenko, *ibid.* **37**, 390 (1983) [**37**, 462 (1983)].

³⁰I. M. Lifshitz and Yu. Kagan, Zh. Eksp. Teor. Fiz. **62**, 385 (1972) [Sov. Phys. JETP. **35**, 462 (1972)].

³¹L. D. Landau and E. M. Lifshitz, Statistical Physics, Part I. Pergamon, 1980.

³²F. V. Kusmartsev and E. I. Rashba, in: Kooperativnye yavleniya (Cooperative Phenomena), Valgus, Tallin, 1982, p. 193.

³³M. C. Cross, Quantum Fluids and Solids, S. B. Trickey *et al.*, eds., Plenum 1977, p. 183.

³⁴T. Suemoto and H. Kanzaki, J. Phys. Soc. Jpn. **50**, 3664 (1981).

³⁵A. V. Sherman, Solid State Commun. **44**, 1253 (1982).

Translated by J. G. Adashko